

# Electronic Supporting Information

## Photoactuation of Micromechanical Devices by Photochromic Molecules

José Elías Angulo-Cervera,<sup>a,b</sup> Mario Piedrahita-Bello,<sup>a,b</sup> Barbora Brachňáková,<sup>a,c</sup> Alejandro Enríquez-Cabrera,<sup>a</sup> Liviu Nicu,<sup>b</sup> Thierry Leichle,<sup>b,d</sup> Fabrice Mathieu,<sup>b</sup> Lucie Routaboul,<sup>a</sup> Lionel Salmon,<sup>a</sup> Gábor Molnár,<sup>a,\*</sup> Azzedine Bousseksou<sup>a,\*</sup>

<sup>a</sup> LCC, CNRS & University of Toulouse, 205 route de Narbonne, 31077 Toulouse, France.

[azzedine.bousseksou@lcc-toulouse.fr](mailto:azzedine.bousseksou@lcc-toulouse.fr), [gabor.molnar@lcc-toulouse.fr](mailto:gabor.molnar@lcc-toulouse.fr)

<sup>b</sup> LAAS, CNRS & University of Toulouse, 7 avenue du Colonel Roche, 31400 Toulouse, France.

<sup>c</sup> Department of Inorganic Chemistry. Faculty of Chemical and Food Technology. Slovak University of Technology in Bratislava. Bratislava SK-81237, Slovakia.

<sup>d</sup> Georgia Tech-CNRS International Research Laboratory, School of Electrical and Computer Engineering, Atlantic Drive, Atlanta, GA, 30332, USA.

## EXPERIMENTAL DETAILS

### Materials

The photochromic molecules 1',3'-Dihydro-1',3',3'-trimethyl-6-nitrospiro[2H-1-benzopyran-2,2'-(2H)-indole] (CAS 1498-88-0) were purchased to Sigma-Aldrich. The copolymer poly(vinylidene fluoride - trifluoro-ethylene) P(VDF<sub>70</sub>-TrFE<sub>30</sub>), with 70-30% monomer ratio was purchased from Piezotech. All chemicals were used as received.

### Substrate cleaning protocol

All the substrates and cantilevers were pre-cleaned by rinsing them in acetone, then in deionized water and finally in ethanol. To remove organic contaminants the substrates were further cleaned in a PVA TePla 300 microwave plasma system with 1 L/min O<sub>2</sub> flow and 800 watts power during 5 minutes. MEMS cantilevers cannot be cleaned in plasma due the hazard of degrading the metallic parts. Instead, a Jelight UVO-Cleaner 42 UV-Ozone cleaning chamber (10 minutes) was employed to remove organic pollution present on the cantilevers.

### Spray coating protocol

The spiropyran powder (0.5 g) and P(VDF-TrFE) (1 g) were dissolved in a mixture of 2-butanone (50 mL) and acetone (100 mL) and spray-coated over silicon and glass substrates using a SUSS MicroTec AltaSpray 8 manual spray coater. The substrates were held at 65 °C to ensure the fast evaporation of the solvent. The film thickness was controlled by adjusting the flow rate through the nozzle (between 1.1 and 3.3 ml/min) leading to 350 nm – 1.2 μm film thickness per spray cycle.

### Sample characterization

Scanning electron microscopy (SEM) imaging was conducted by means of a HITACHI S-4800 electronic microscope with an acceleration range between 0.5 kV and 2 kV and mean current of 1 μA. Atomic force microscopy (AFM) surface topography images were acquired with an Asylum Research Cypher ES in amplitude modulation mode. Grazing incidence X-ray diffraction (GIXRD) measurements were conducted using a PANanalytical X'Pert PRO MPD system in a parallel beam configuration; the X-Ray source is a Cu-K<sub>α</sub> radiation. Fourier-transform infrared (FTIR) spectra were recorded Perkin-Elmer Spectrum Two spectrometer in ATR configuration. The absorbance of the films was recorded using a Cary 50 (Agilent) UV-Vis spectrophotometer in the wavelength range between 300 and 1000 nm. A THMS-600 (Linkam Scientific) heating-cooling stage was used to control the sample temperature.

### MEMS characterization

The MEMS used here were the same as described by Manrique-Juarez in Adv. Funct. Mater. vol. 28, no. 29, p. 1801970, 2018. The dynamic and static behaviors of the cantilevers were tracked simultaneously. For the dynamic measurements, the device was actuated at its resonance frequency by means of the Lorentz force *via* an external magnetic field. The mechanical stress induced by the vibration of the cantilever was detected by piezoresistors, which are integrated at the clamping zone. A homemade, vector network analyzer based, system was used to detect the piezoresistance changes and to assess the resonance frequency ( $f_r$ ) and the quality factor ( $Q$ ) of the cantilever. A reference cantilever was also included into the chip design to compensate the drifts in the measurements. To quantify the amplitude of the cantilever tip deflection ( $\delta$ ), we used the static piezoresistance signal, which was calibrated using an optical vibrometer. The measurements were conducted at a controlled temperature and constant vacuum pressure of 10 mbar, which allows for high quality factors (by decreasing the air damping) and shunts parasitic signals due to changes in the environmental conditions (e.g. humidity).

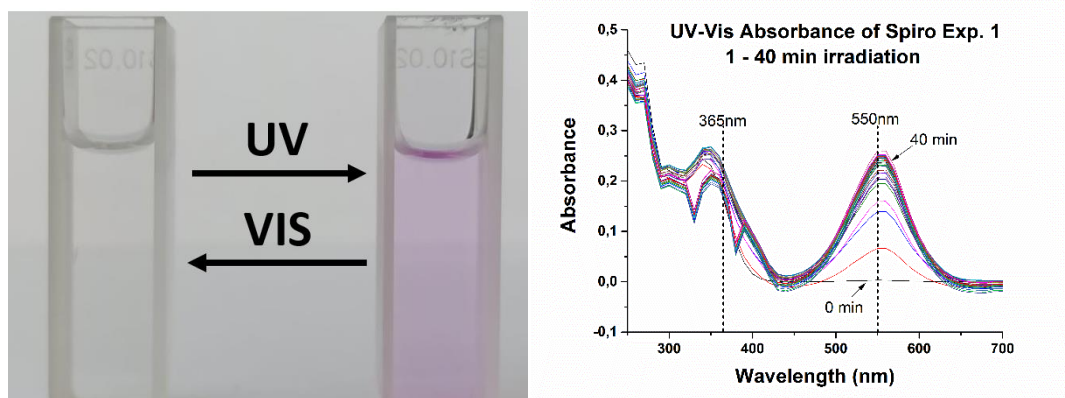


**Fig. S1. Left:** Photochromic properties of the spiropyran molecule in acetonitrile at room temperature. **Right:** Solution study of spiropyran ( $10^{-5} \text{ mol}\cdot\text{dm}^{-3}$ ) upon UV irradiation over 40 min in acetonitrile.

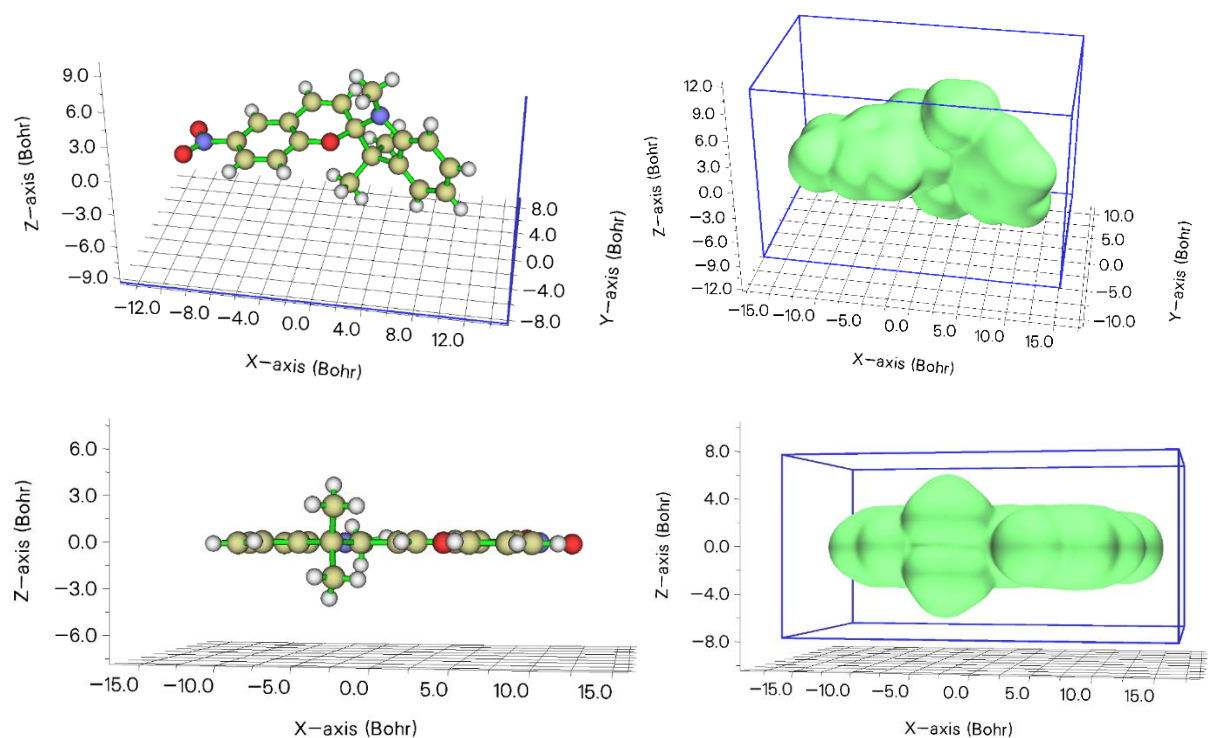


**Fig. S2. Top panel:** Calculated structure and volume ( $362 \text{ \AA}^3$ ) of the closed-ring spiropyran isomer. **Bottom panel:** Calculated structure and volume ( $366 \text{ \AA}^3$ ) of the open-ring merocyanine isomer. Structure optimization and calculation of the molecular volume (defined as the volume inside a contour of  $0.001 \text{ electrons/Bohr}^3$  density) were performed in the Multiwfn software (Tian Lu, Feiwu Chen, Multiwfn: A Multifunctional Wavefunction Analyzer, *J. Comput. Chem.* 33, 580-592 (2012) DOI: 10.1002/jcc.22885) by means of the Quantitative molecular surface analysis module (Tian Lu, Feiwu Chen, Quantitative analysis of molecular surface based on improved Marching Tetrahedra algorithm, *J. Mol. Graph. Model.*, 38, 314-323 (2012) DOI: 10.1016/j.jmgm.2012.07.004)

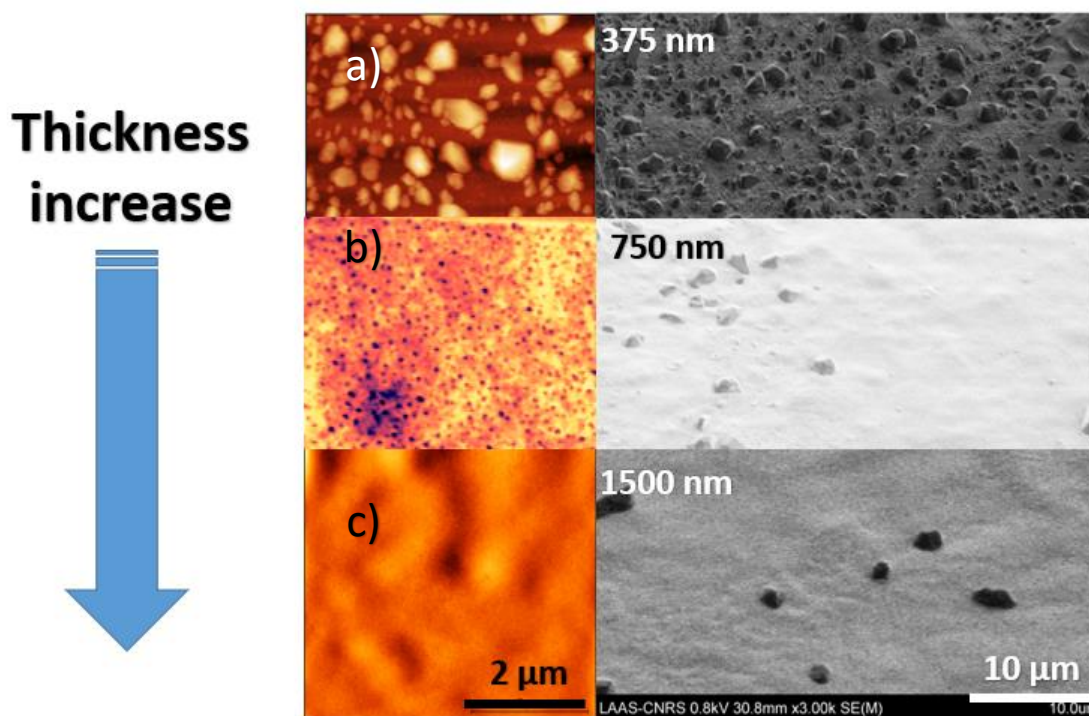


**Fig. S3.** SP microcrystals formed during the spray coating of the composite films over a clean Si substrate. **Left:** AFM images. **Right:** SEM images for a) 375 nm thickness (1 coating cycle), b) 750 nm thickness (2 coating cycles) and c) 1500 nm thickness (4 coating cycles). As the number of deposition cycles increases, the density of the formed crystals radically decreases.

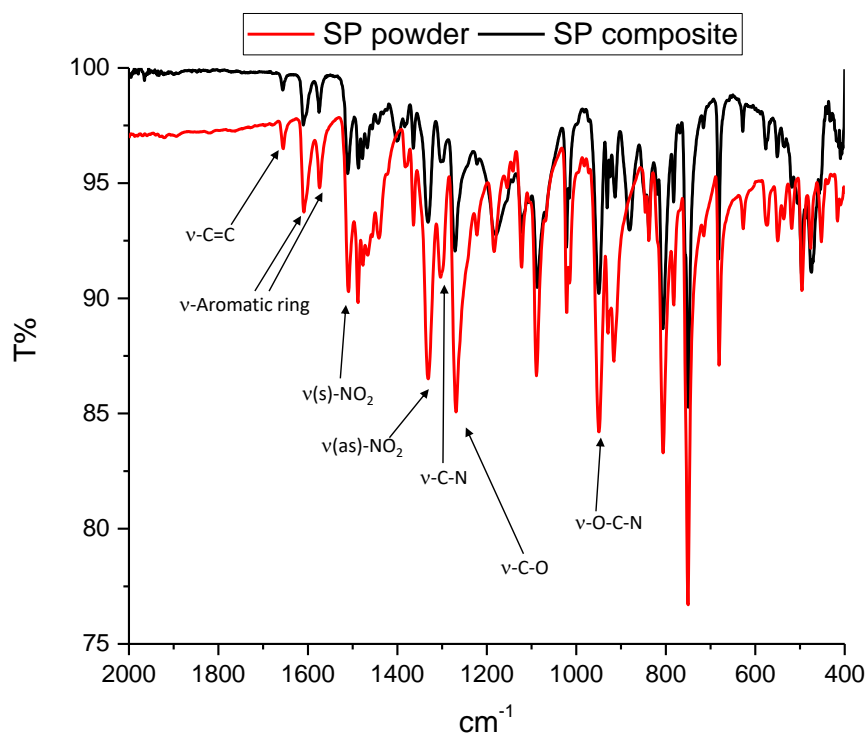


**Fig. S4.** FTIR fingerprint spectra of the pure spiropyran powder and a composite film.



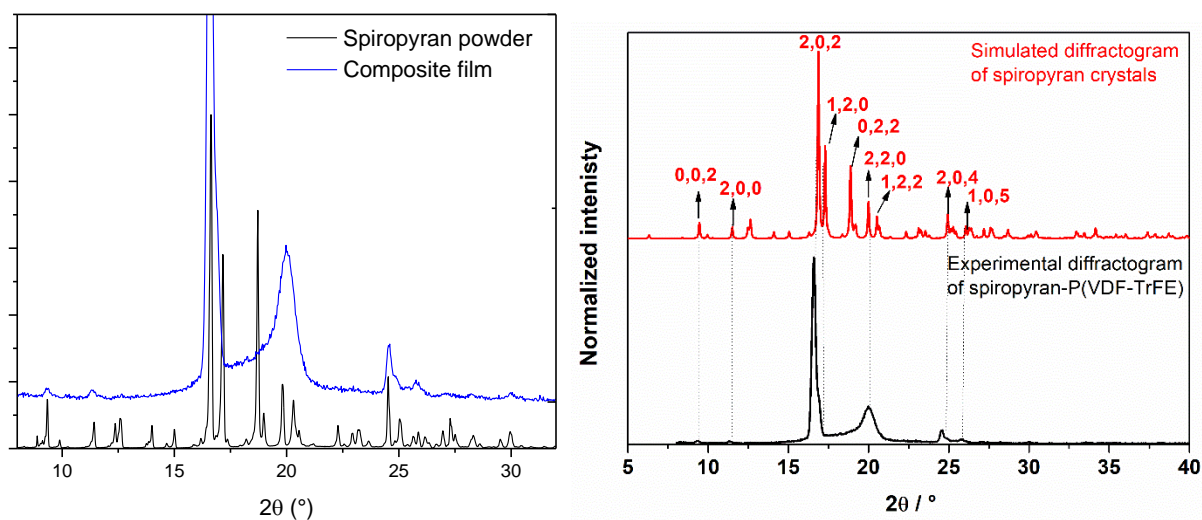


**Fig. S5. Left.** Comparison of x-ray diffractograms on spiropyran powder and a composite film (acquired in grazing incidence). The broad peak in the diffractogram of the composite around  $20^\circ$  is due to the (semi)crystalline polymer matrix. The intense peak at  $16.8^\circ$  has been indexed to the 202 reflection, denoting a preferential orientation of the spiropyran crystallites within the matrix. **Right.** Powder x-ray diffractogram of spiropyran calculated from the single-crystal structure.

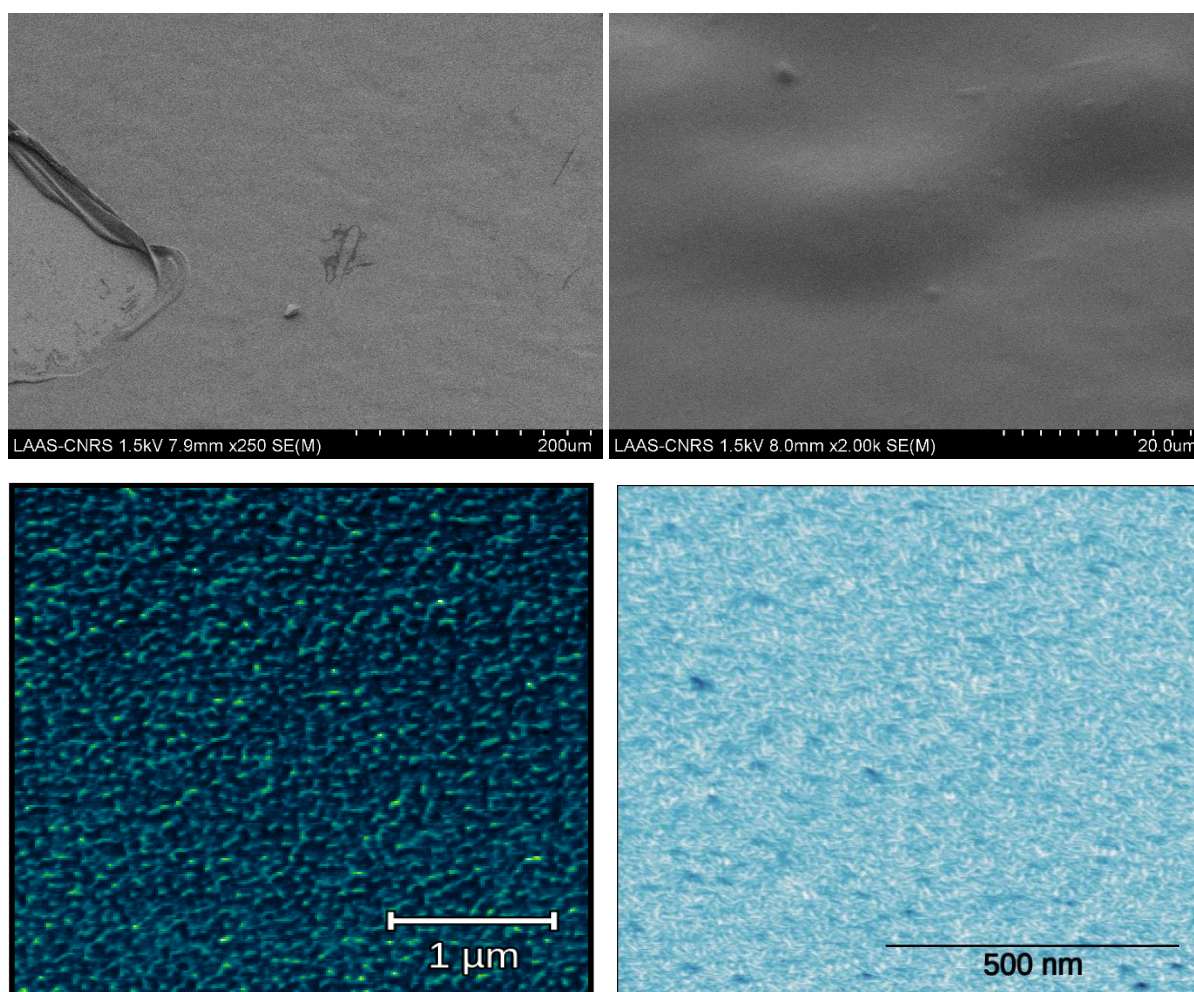


**Fig. S6. Top** - SEM and **Bottom** - AFM phase images (tapping mode) of a composite film surface.

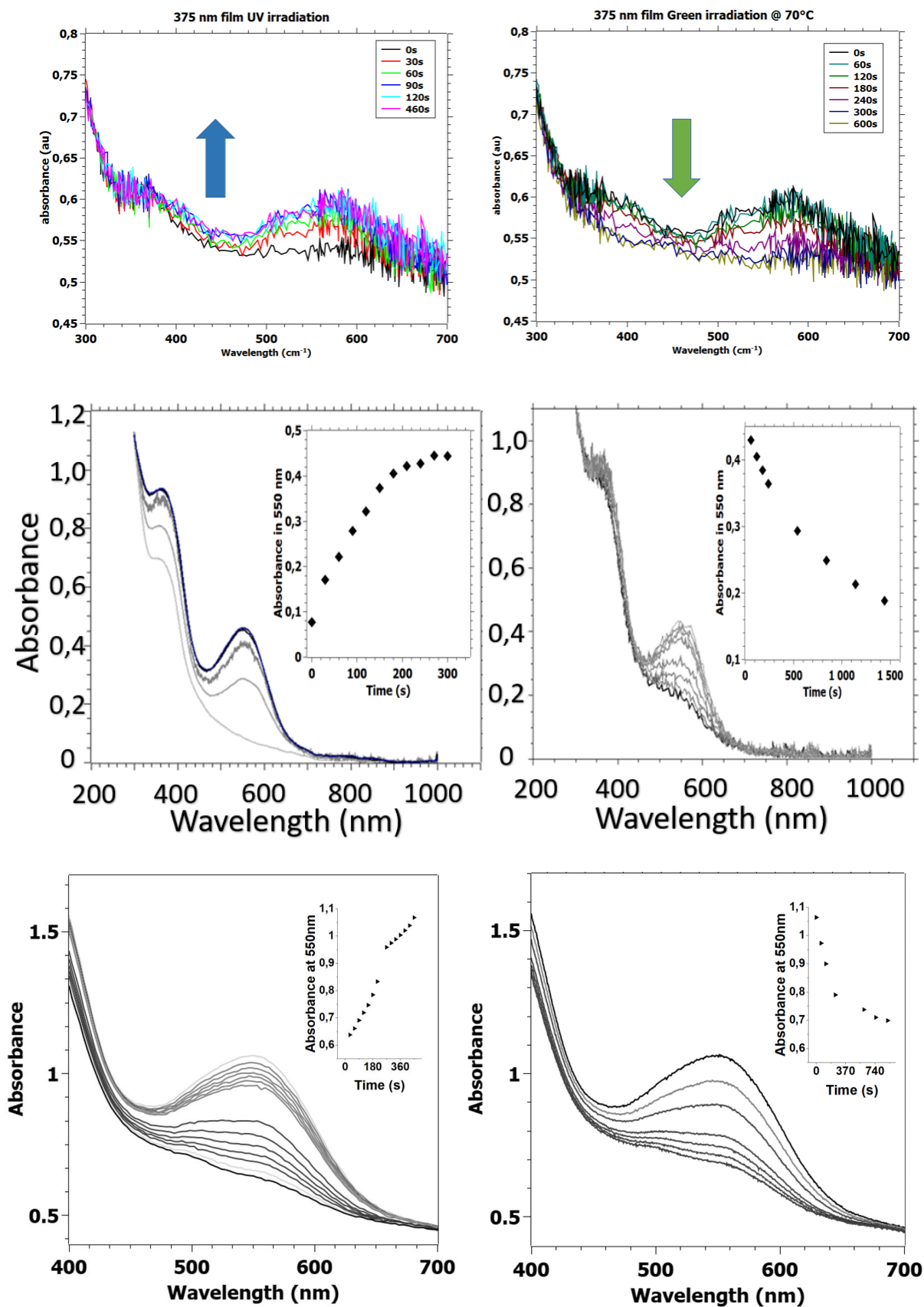


**Fig. S7.** UV-VIS absorption spectra of a 375 nm (TOP), 750 nm (MIDDLE) and 1500 nm (BOTTOM) thick spiropyran@P(VDF-TrFE) film upon UV light (LEFT) and visible light (RIGHT) irradiation. Irradiations with UV and visible light were conducted at 20 °C and 70 °C, respectively.

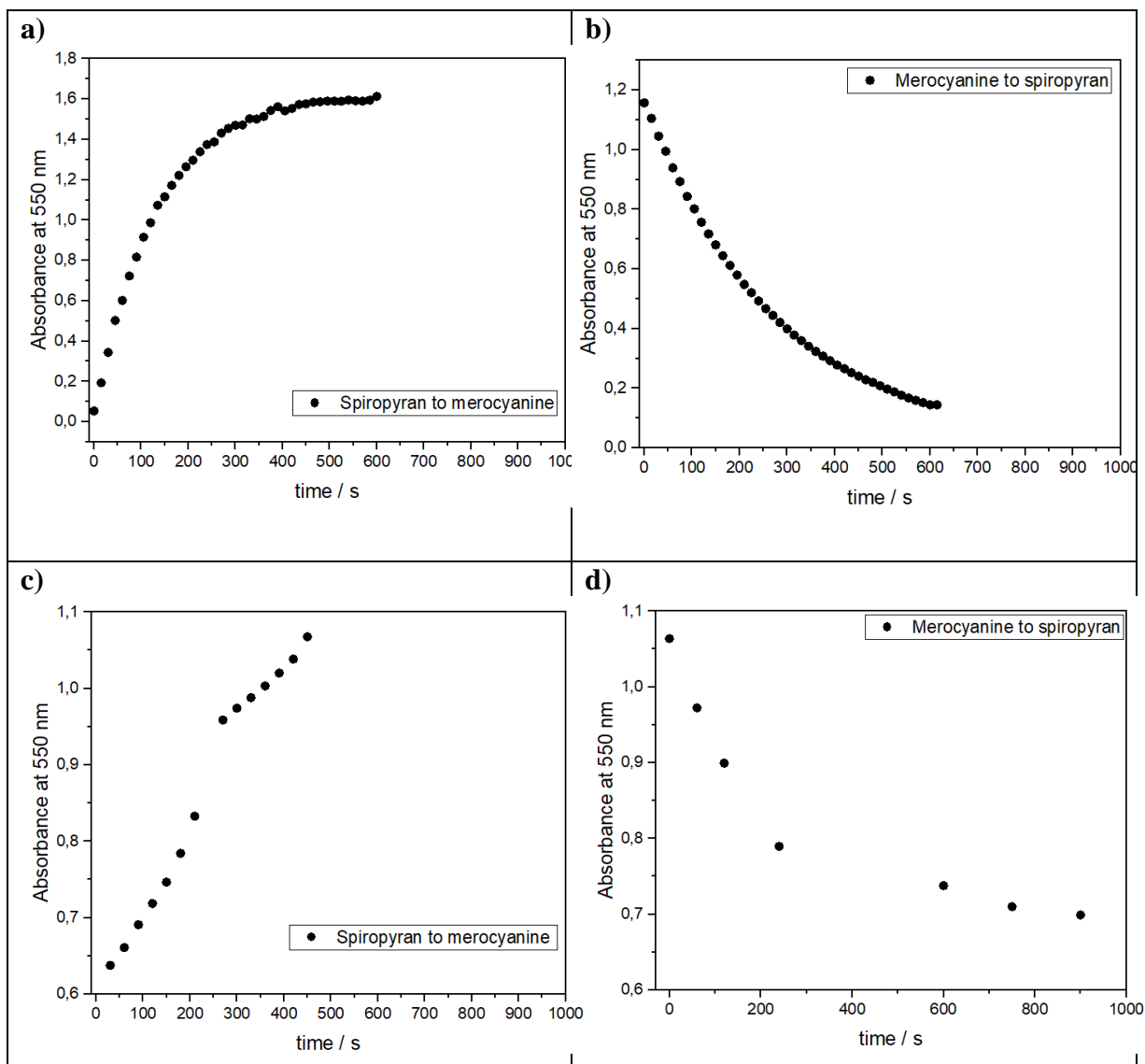


**Fig. S8.** Reversible conversion between spiropyran and merocyanine is displayed as time dependence of absorbance at 550 nm for solution (a and b) and for a 1550 nm thick spiropyran@P(VDF-TrFE) film (c and d). The spiropyran solution ( $c=1.10^{-4}$  mol.dm<sup>-3</sup>, acetonitrile) was irradiated by 365 nm light for 600 seconds and the conversion from merocyanine to spiropyran form was achieved by 565 nm irradiation for 600 seconds. Spectra were collected every 15 seconds during continuous light irradiation.

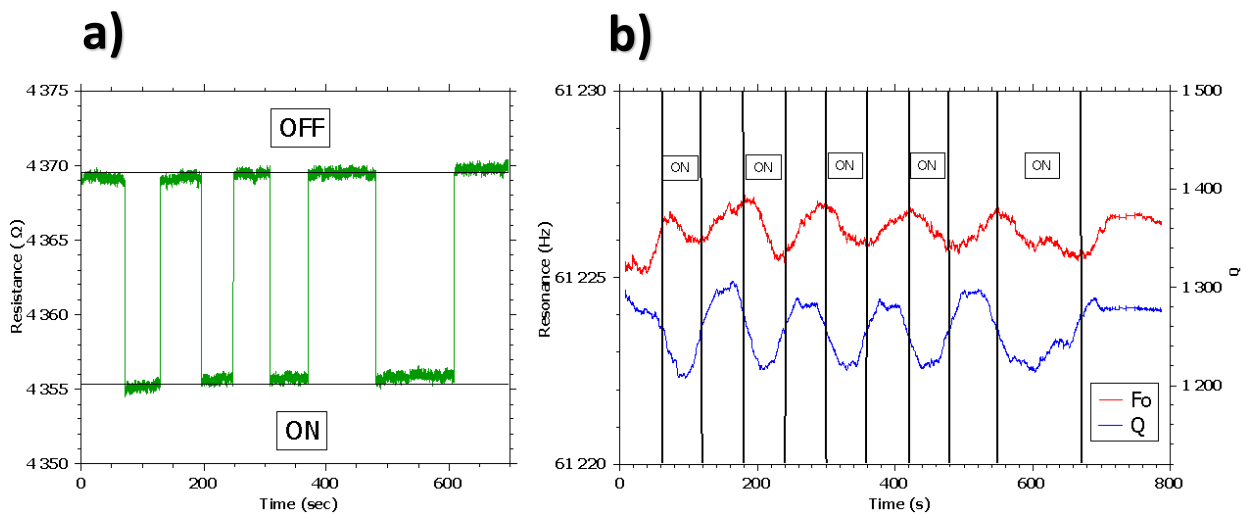


**Fig. S9.** ON-OFF irradiation cycles (530 nm) of the uncoated cantilever. a) Static piezoresistance, b) resonance frequency (red) and Q factor (blue).

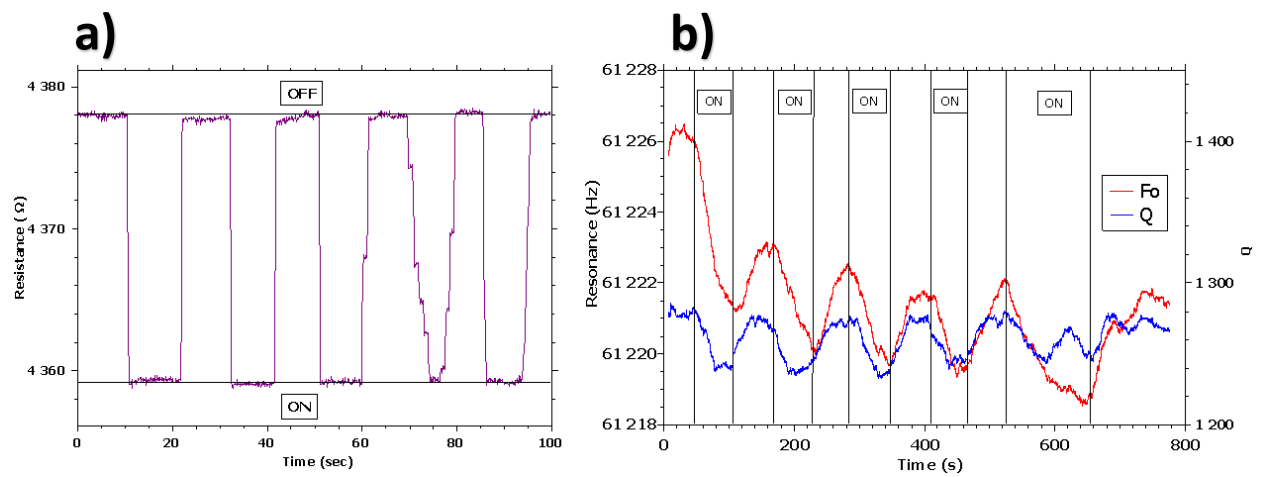


**Fig. S10.** ON-OFF irradiation cycles (350 nm) of the uncoated cantilever. a) Static piezoresistance, b) resonance frequency (red) and Q factor (blue).



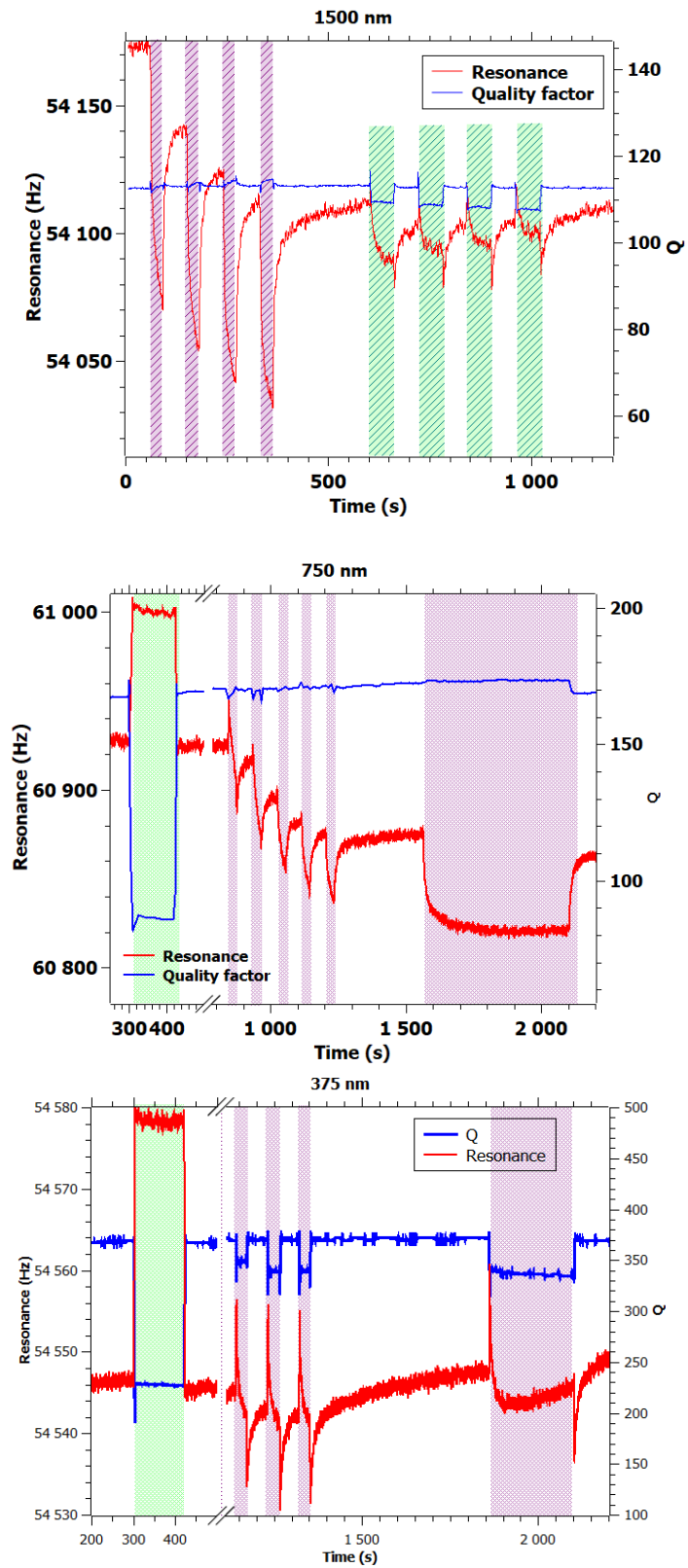


**Fig. S11.** MEMS resonance frequency tracking for the 375, 750 and 1500 nm thick films at room temperature. The green and the purple zones correspond to 530 and 350 nm irradiation, respectively.

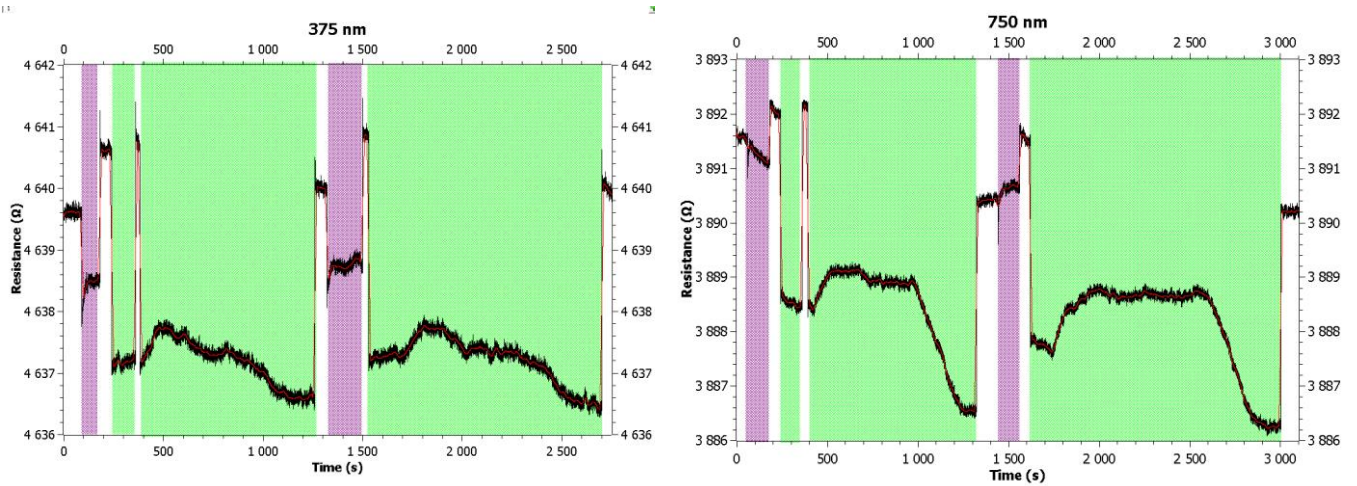
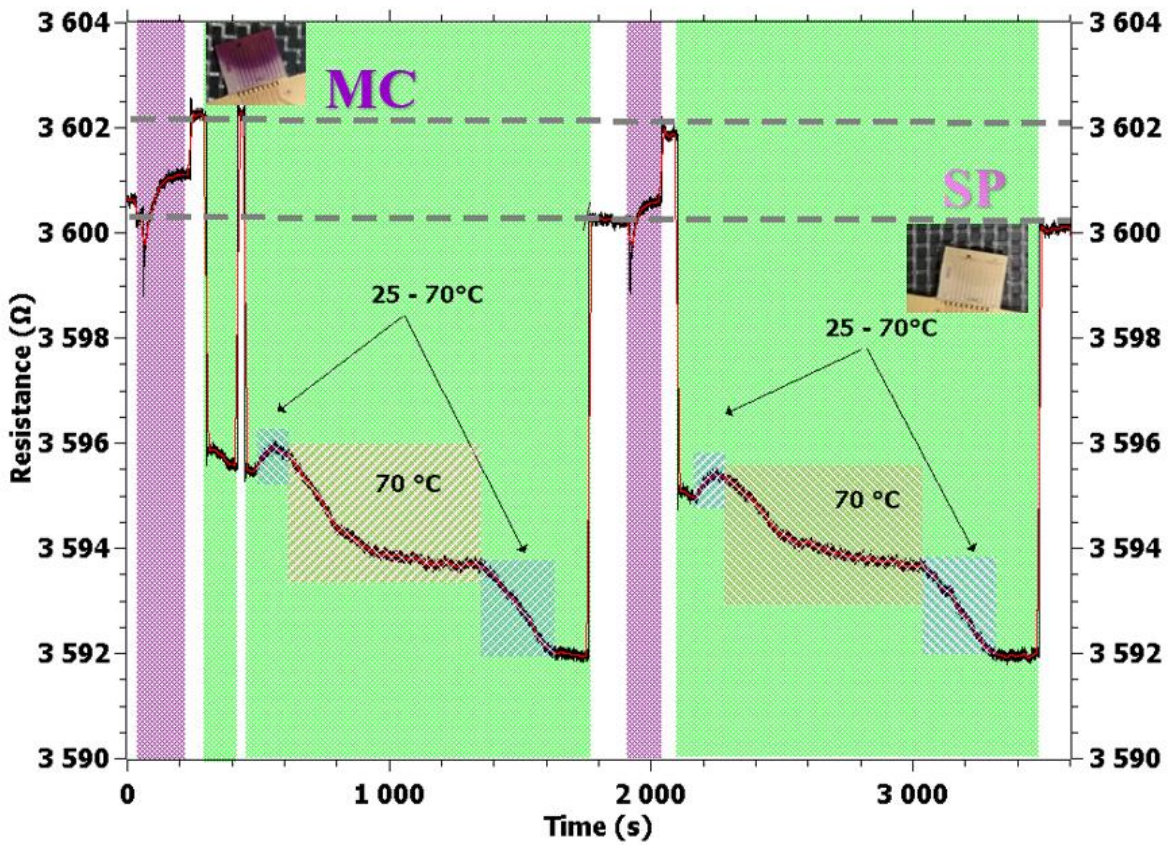


**FIG. S12.** MEMS static piezoresistance tracking. **TOP:** Irradiation cycling of the 1500 nm film. The purple (green) zone corresponds to 350 (530) nm irradiation. Blue patterns indicate heating-cooling ramps and the red patterns refer to constant 70 °C. The photographs in insert show the MEMS device before and after the erasing procedure. **BOTTOM:** Similar static piezoresistance tracking data for the 375 and 750 nm thick composite films.

Film thickness (nm)	375	750	1500
Tip displacement (nm)	150	200	349
Cantilever curvature (1/nm)	1.3E-08	1.8E-08	3.4E-08
Strain (%)	0.16	0.11	0.10
Stress (MPa)	5.1	3.4	3.2
W/V (mJ/cm <sup>3</sup> )	3.6	1.8	1.6

**Table S1.** Actuation parameters extracted for the composite films of different thickness